J Mater Sci (2008) 43:2053–2057
DOI 10.1007/s10853-007-2424-x

Synthesis of hexagonal $Al_{2-x}Cr_xO_3$ nanodisks by a thermal decomposition of mesoporous Cr^{4+}:Al_2O_3 powders

Paritosh Mohanty · Shanker Ram

Received: 17 April 2007 / Accepted: 17 December 2007 / Published online: 31 January 2008

Abstract Monodispersed hexagonal $Al_{2-x}Cr_xO_3$ nanodisks are synthesized through a reactive doping of Cr^{6+} cations in a hydrogenated mesoporous $AlO(OH)\cdot\alpha H_2O$ powder followed by annealing at 1,200 °C in air. The reaction was carried out by a drop wise addition of an aqueous Cr^{6+} solution (0.5–1.0 M) to $AlO(OH)\cdot\alpha H_2O$, at room temperature. $Al_{2-x}Cr_xO_3$ nanostructure formation was controlled by the nucleation and growth from the intermediate amorphous mesoporous Cr^{4+}:Al_2O_3 composites in the temperature range 400–1,000 °C. The nanodisks of ~50 nm diameter and thickness of ~16 nm is observed in the sample with x of 0.2 and similar nanodisks with a low dimension is observed at a higher value of x of 1.6 (after 2 h of heating at 1,200 °C). The $Cr^{3+} \leftrightarrow Al^{3+}$ substitution, $x \leq 1.2$, inhibits grain growth in small crystallites. The crystallites in $x = 0.2$ composition have 43 nm diameter while it is 15 nm in those with $x = 1.2$ composition.

Introduction

The electronic, optical as well as other properties of a particle depends on its particular size, shape, and local dielectric environment [1, 2]. Nanostructures of controlled size and shape is important in controlling their chemical and physical properties due to quantum size effect [3, 4]. As an insulator with a wide band gap, alumina itself provides a good matrix to implanting various ions that has good prospects to achieve emitting properties. The substitution of Al^{3+} with Cr^{3+} forms an isovalent $Al_{2-x}Cr_xO_3$ series of an important class of optical materials because of its promising fluorescence properties as lasers [5–7]. The high refractoriness and chemical stability of $Al_{2-x}Cr_xO_3$ series offers many applications in energy plants [8] to pose superior corrosion resistance against molten salts attacks [9, 10].

Both Cr_2O_3 and α-Al_2O_3 are sesquioxides, with $R\bar{3}c$ hexagonal corundum crystal structure [11]. In this crystal structure, the metal cations occupy two-thirds of the octahedral interstitial sites. The properties can be modified in the $Al_{2-x}Cr_xO_3$ series depending on the x-value. The linearity in change of lattice parameters of such $Al_{2-x}Cr_xO_3$ systems as a function of x according to the Vegard's law [12, 13] is debatable. A miscibility dome exists in Al_2O_3 rich and Cr_2O_3 rich crystalline phases at temperatures below 950 °C [8, 11]. Reaction above 1,000 °C results in the formation of isomorphous $Al_{2-x}Cr_xO_3$ substitutional solid solution [8, 11]. Therefore, there is a growing interest in nonconventional solid-state methods of synthesis of $Al_{2-x}Cr_xO_3$ at low temperature in shorter times. Wet chemical methods are preferred to obtain a molecular homogeneity that in turn enables shorter average ionic diffusion paths at high reaction rate [8, 14, 15]. However, all the above reports of the synthesis of the $Al_{2-x}Cr_xO_3$ are confined to the bulk materials. To the best of our knowledge no report is available on the synthesis of isomorphous $Al_{2-x}Cr_xO_3$ in nanostructures. In this article, we report the synthesis of monodispersed isomorphous $Al_{2-x}Cr_xO_3$ nanodisks through a novel wet chemical route

P. Mohanty · S. Ram
Material Science Centre, Indian Institute of Technology, Kharagpur, Kharagpur 721302, India

Present Address:
P. Mohanty (✉)
Department of Chemistry, Lehigh University, Bethlehem, PA 18015, USA
e-mail: pam206@lehigh.edu

by the reaction of Cr^{6+} with a hydrogenated mesoporous $AlO(OH)\cdot\alpha H_2O$ powder.

Experimental details

The synthesis of $Al_{2-x}Cr_xO_3$ ($0.2 \leq x \leq 1.6$) is carried out by a reaction of Cr^{6+} cations with a hydrogenated mesoporous $AlO(OH)\cdot\alpha H_2O$, $\alpha = 0.25$, powder followed by annealing in the temperature range 400–1,200 °C in air. This involves a drop wise addition of an aqueous $(NH_4)_2Cr_2O_7$ solution (0.5–1.0 M) to $AlO(OH)\cdot\alpha H_2O$ at room temperature. An intermediate amorphous Cr^{4+}:Al_2O_3 product forms on drying the mixture after the reaction at 150 °C in air. It has a characteristic grayish-black to black color depending on the x-value. A freshly prepared $AlO(OH)\cdot\alpha H_2O$, with an initial porosity of ~90% and 10–50 nm average pore diameter, was used. It was obtained by an electrochemical surface hydrolysis of Al-metal in a humid air [16–18].

Phase analysis of the samples before and after the reaction at selected temperatures is carried out with X-ray diffraction (XRD). The diffraction has been recorded with P. W. 1710 diffractometer operated at 40 kV voltage and 20 mA current using filtered CoK_∞ radiation of 0.17905 nm wavelength. Desorption of chemisorbed gases, thermal decomposition and nucleation and growth of $Al_{2-x}Cr_xO_3$ from the precursor powder were studied with differential scanning calorimetry (DSC) and thermogravimetric analysis (TG). A Perkin-Elmer thermal analyzer was used to record the two curves by heating 10–20 mg sample in the 30–600 °C range in air at 20 °C/min heating rate. Transmission electron microscope (TEM) images were collected on a Philips CM12 microscope at an accelerating voltage of 120 kV. The sample for the TEM studies is prepared from powder dispersed in an organic solvent and then a drop of it was put over a carbon-coated copper grid.

Results and discussion

Reaction process

The hydrogenated mesoporous $AlO(OH)\cdot\alpha H_2O$ powder behaves as a reducing agent. It converts Cr^{6+} to Cr^{4+} as soon as it is added and dispersed in the mesopores. This is an exothermic reaction which can be seen by 5–10 °C increase in average temperature of the mixture as per the experimental conditions. The local temperature in the reaction centers may be higher, i.e., sufficient to cause in-situ $AlO(OH)\cdot\alpha H_2O \rightarrow Al_2O_3$ molecular decomposition [16–18]. The reaction with energized $AlO(OH)\cdot\alpha H_2O$ in the mesopores, which involve a high surface energy, thus can be expressed as,

$$(NH_4)_2Cr_2O_7 + 2H_2 + 2AlO(OH) \rightarrow 2CrO_2 + Al_2O_3 + 2NH_3 + 4H_2O \quad (1)$$

The product in this reaction results with formation of an intermediate amorphous Cr^{4+}:Al_2O_3 phase. This amorphous phase is annealed at selected temperatures to produce the nanocrystalline phase of the isomorphous $Al_{2-x}Cr_xO_3$ compound.

Formation of $Al_{2-x}Cr_xO_3$ ($0.2 \leq x \leq 1.6$) nanostructures

The obtained metastable mesoporous Cr^{4+}:Al_2O_3 precursors have an amorphous structure which can be analyzed by its XRD. For example, typical X-ray diffractograms are shown in Fig. 1 at x of (a) 0.2 and (b) 0.8. It consists of distinct broad halos. The halos describe an amorphous structure of the Cr^{4+}:Al_2O_3 specimen [19–21]. A resolved halo q_1 appears at (a) 18 or (b) 19 nm^{-1}. Another halo q_2 (weak) lies at 44 nm^{-1} in sample (a). A well-resolved distribution of pores through the particles in a mesoporous structure lies in Cr^{4+}:Al_2O_3 precursor powder. This is demonstrated with TEM micrograph in a typical sample of x of 1.6 in the inset to Fig. 1. The particles in blackish characteristic contrasts are self-assembled in a network structure through pores in whitish characteristic contrasts. They are in shape of elongated platelets or rods of an average 6–10 nm diameter and 10–20 nm length. Those are interconnected in a specific network to form a peculiar mesoporous structure in which the pores and particles are

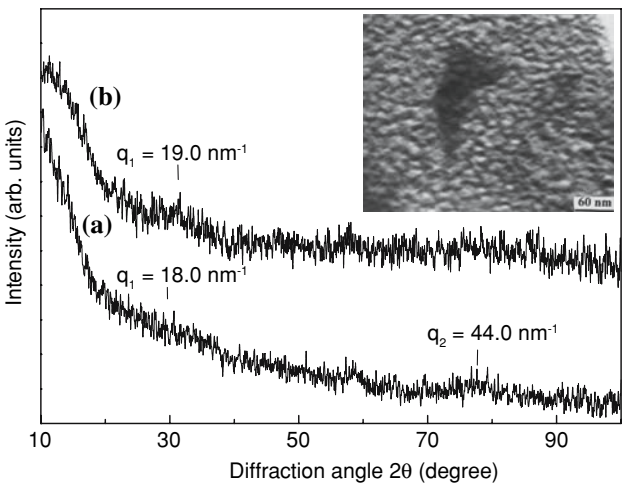

Fig. 1 X-ray diffractograms in Cr^{4+}:Al_2O_3 precursor powders (dried at 450 K) showing the amorphous nature of the specimens with the value of x of (**a**) 0.2 and (**b**) 0.8. A TEM image is given in the inset demonstrates the mesoporous structure of the precursor powder

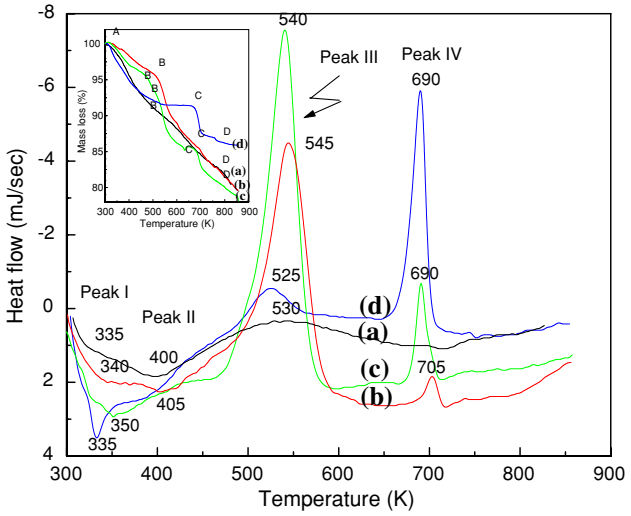

Fig. 2 DSC thermograms in mesoporous Cr^{4+}:Al_2O_3 powders (dried at 450 K) at a heating rate of 20 K/min; (**a**) 10, (**b**) 40, (**c**) 60, and (**d**) 80 mol.% of Cr^{3+}. The inset shows TGA thermograms in the respective samples

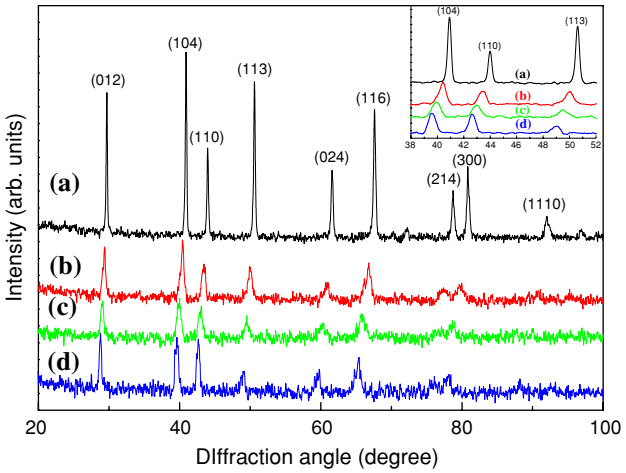

Fig. 3 X-ray diffractograms in $Al_{2-x}Cr_xO_3$ nanoparticles obtained in 2 h of heating at 1,200 °C from mesoporous Cr^{4+}:Al_2O_3 powders of x of (**a**) 0.2, (**b**) 0.8, (**c**) 1.2, and (**d**) 1.6. The inset shows the regular shifts in (104), (110), and (113) peaks

intimately interrelated one another with a strong macroscopic interaction. Average pore size in this fine structure varies at a scale of 10–20 nm.

Nucleation and growth in the $Al_{2-x}Cr_xO_3$ nanostructures occurs from the amorphous Cr^{4+}:Al_2O_3 precursors on heating at 400–1,000 °C in air. Figure 2 shows the DSC curves for the precursor powders of x of (a) 0.2, (b) 0.8 (c) 1.2 and (d) 1.6. Two endothermic signals of A and B ascribe desorption of chemisorbed species of NH_3 and O_2 (or CO_2) gases and moisture [17, 18]. The NH_3 and O_2 (or CO_2) molecules occupying the pores release easily at low temperature primarily in signal A. The peak at B arises due to desorption of the residual gases with H_2O molecules from the particle surfaces. These gases easily adsorb in association with H_2O molecules and exist at high-energy surfaces up to rather high temperatures. Both the signals extend to a maximum of 200 °C. This is well demonstrated from loss in mass of the specimen in TG curve in the inset to Fig. 3. The $Cr^{4+} \rightarrow Cr^{3+}$ conversion and the nucleation and growth of $Al_{2-x}Cr_xO_3$ in nanoparticles are reflected in two exothermic peaks of C and D (Fig. 2), respectively. Thermograms in Fig. 2 or the inset differ one another in difference of the porosity and other structural parameters.

Annealing at 1,200 °C for 2 h results in a crystalline $Al_{2-x}Cr_xO_3$ powder irrespective of the x-value. For example, Fig. 3 shows XRD from $Al_{2-x}Cr_xO_3$ samples with x equal to (a) 0.2, (b) 0.8, (c) 1.2 and (d) 1.6. All the peaks are indexed assuming the $R\bar{3}c$ corundum crystal structure. The inset in Fig. 3 compares a regular shift in (104), (110) and (113) peaks with x in a continuous phase formation. As analyzed also with other peaks, it reveals a linear increase in the d_{hkl} value (interplanar spacing) with a linear increase in lattice parameters a or c as a function of x in the Vegard's law [12, 13]. The $Cr^{3+} \rightarrow Al^{3+}$ substitution, $x \leq 1.2$, inhibits the grain growth. The crystallites in $x = 0.2$ composition thus have 43 nm diameter while it is 15 nm in those with $x = 1.2$ composition (after 2 h of heating at 1,200 °C). Other details of the crystallite size, lattice parameters, lattice volume and lattice surface area are given in Table 1 in the various samples.

It is observed that the microstructure varies in recrystallized $Al_{2-x}Cr_xO_3$ powders with a function of the Cr^{3+} contents. This has been studied in detail with TEM micrographs in the samples of selected Cr^{3+} contents in the corundum structure as processed in 2 h of heating at 1,200 °C. For example, Fig. 4a or b shows a typical TEM micrograph in $Al_{2-x}Cr_xO_3$ nanodisks at the value of $x = 0.2$. Micrograph (a) represents a homogeneous distribution of crystallites of hexagonal morphology of 40–50 nm size. Hexagonal discs are clearly seen in a close-up of micrograph inset to (a). Average width of the nanodisks is $\sim$16 nm as

Table 1 Crystallite size D, lattice parameters, lattice volume V_0, and lattice surface area S_0 in $Al_{2-x}Cr_xO_3$ nanocrystals at different x-values after 2 h of heating at 1,200 °C from mesoporous Cr^{4+}:Al_2O_3 precursor powders

x	D (nm)	Lattice parameters (nm)		V_0 (nm^3)	S_0 (nm^2)
		a	c		
0.2	38	0.4784	1.3024	0.7744	4.9276
0.4	32	0.4802	1.3063	0.7826	4.9619
0.6	22	0.4822	1.3101	0.7914	4.9986
0.8	17	0.4842	1.3150	0.8010	5.0386
1.2	15	0.4882	1.3265	0.8214	5.1240
1.6	20	0.4920	1.3404	0.8430	5.2147

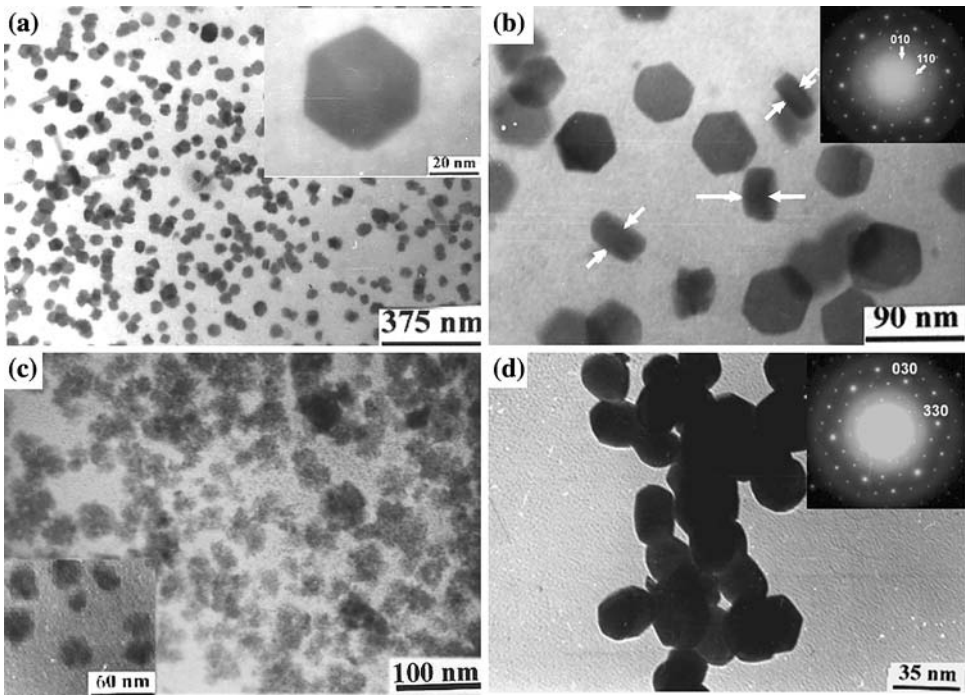

Fig. 4 TEM micrographs in $Al_{2-x}Cr_xO_3$ nanostructures with x of (**a**) or (**b**) 0.2, (**c**) 1.2, and (**d**) 1.6 in 2 h of heating at 1,200 °C. The inset to (**a**) shows a single nanodisk and the corresponding electron diffractogram is shown in the inset to (**b**). Inset to (**c**) shows the nanoparticles of irregular shapes at x of 0.8. The selected area diffraction pattern of $Al_{2-x}Cr_xO_3$, $x = 1.6$, nanodisks is shown in the inset to (**d**)

marked with the arrows in micrograph (b). The electron diffractogram (inset) corresponding to micrograph (b) has well defined arrays of diffraction spots from arrays of lattice planes in the corundum $Al_{2-x}Cr_xO_3$ structure demonstrating the single crystalline nature of the specimen. A similar microstructure of hexagonal nanodisks is observed in the Cr^{3+} rich sample. This is shown in the micrograph in Fig. 4d with the value of x of 1.6. At such concentration of Cr^{3+} the nanodisks are rather small in size as small as 20 nm. The corresponding electron diffractogram as shown in the inset to (d) is similar as in the other specimen (b) demonstrating that both the obtained specimen are single crystalline in nature. Such nanodisks are also reported in several other systems such as silver, cadmium, ZnO, rare earth oxides, etc [22–25].

At a moderate chromium concentration, x of 0.8 or 1.2, the hexagonal nanodisks morphology of isomorphous $Al_{2-x}Cr_xO_3$ changes to nearly cubical or spherical ones as shown in the inset or Fig. 4c. In these samples a peculiar mesoporous $Al_{2-x}Cr_xO_3$ structure develops a strong mixing between small particles and pores. The particles of 15–30 nm diameter are distributed through 10–20 nm pores.

Conclusions

A reactive doping of Cr^{6+} cations in a mesoporous $AlO(OH)\cdot\alpha H_2O$ precursor powder results in $Al_{2-x}Cr_xO_3$ nanostructures, 15–45 nm diameter, following annealing at 1,200 °C in air. A continuous solid $Al_{2-x}Cr_xO_3$ solution is obtained in this case. The morphology is strongly dependent on the concentration of Cr^{3+}. Hexagonal $Al_{2-x}Cr_xO_3$ nanodisks are formed at a low ($x = 0.2$) as well as high ($x = 1.6$) Cr^{3+} contents. A peculiar mesoporous $Al_{2-x}Cr_xO_3$ structure is observed at a moderate value of x of 0.8 or 1.2 in a strong mixing between small particles and pores.

Acknowledgement This work has been financially supported by the Council of Scientific & Industrial Research (CSIR) and the Defense Research & Development Organization (DRDO), Government of India.

References

1. Aizpurua J, Hanarp P, Sutherland DS, Käll M, Bryant GW, García de Abajo FJ (2003) Phys Rev Lett 90:57401
2. Li F, Ding Y, Gao P, Xin X, Wang ZL (2004) Angew Chem Int Ed 43:5238
3. Li F, He J, Zhou W, Wiley JB (2003) J Am Chem Soc 125:16166
4. Li F, Xu L, Zhou WL, He J, Baughman RH, Zakhidov AA, Wiley JB (2002) Adv Mater 14:1528
5. Maiman TH (1960) Nature 173:493
6. Wen Q, Lipkin DM, Clarke DR (1998) J Am Ceram Soc 81:3345
7. Yu H, Clarke DR (2002) J Am Ceram Soc 85:1966
8. Bondioli F, Ferrari AM, Leonelli C, Manfredini T, Linati L, Mustarelli P (2000) J Am Ceram Soc 83:2036
9. Grabke HJ (1994) In: Nickel KG (ed) Corrosion of advanced ceramics measurement and modelling. Kluwer Academic, Dordrecht, p 223
10. Rapp RA (1989) In: Johannesen O (ed) Selected topics in high temperature chemistry: defect chemistry of solids. Elsevier, p 291
11. Roy DM, Barks RE (1972) Nature Phys Sci 235:118
12. Spriggs RM, Bender Sl (1962) J Am Ceram Soc 45:506
13. Rossi LR, Lawrence WG (1970) J Am Ceram Soc 53:604

14. Hirata T, Akiyama K, Yamamoto H (2000) J Eur Ceram Soc 20:195
15. Kim SS, Sanders TH Jr (2001) J Am Ceram Soc 84:1881
16. Ram S (2003) J Am Ceram Soc 86:2037
17. Mohanty P, Ram S (2002) Phil Mag B 82:1129
18. Mohanty P, Ram S (2003) J Mater Chem 13:3021
19. Azaroff L (1968) Elements of X-ray crystallography. McGraw-Hill, New York
20. Chen LC, Spaepen F (1988) Nature 336:366
21. Ram S, Joubert JC (1991) Phys Rev B 44:6825
22. Li F, Ding Y, Gao P, Xin X, Wang ZL (2004) Angew Chem Int Ed 43:5238
23. Si R, Zhang YW, You LP, Yan CH (2005) Angew Chem Int Ed 44:3256
24. Germian V, Brioude A, Ingert D, Pileni MP (2005) J Chem Phys 122:124707
25. Mohanty P, Park J, Lee G, Kim B (2006) J Nanosci Nanotechnol 6:3376